Distinct regulation of Ubc13 functions by the two ubiquitin-conjugating enzyme variants Mms2 and Uev1A

Parker L. Andersen,[1] Honglin Zhou,[2] Landon Pastushok,[1] Trevor Moraes,[3] Sean McKenna,[3] Barry Ziola,[4] Michael J. Ellison,[3] Vishva M. Dixit,[2] and Wei Xiao[1]

[1]Department of Microbiology and Immunology and [4]Department of Pathology, University of Saskatchewan, Saskatoon, Saskatchewan S7N 5E5, Canada
[2]Department of Molecular Oncology, Genentech Inc., South San Francisco, CA 94080
[3]Department of Biochemistry, University of Alberta, Edmonton, Alberta T6G 2H7, Canada

Ubc13, a ubiquitin-conjugating enzyme (Ubc), requires the presence of a Ubc variant (Uev) for polyubiquitination. Uevs, although resembling Ubc in sequence and structure, lack the active site cysteine residue and are catalytically inactive. The yeast Uev (Mms2) incites noncanonical Lys63-linked polyubiquitination by Ubc13, whereas the increased diversity of Uevs in higher eukaryotes suggests an unexpected complication in ubiquitination. In this study, we demonstrate that divergent activities of mammalian Ubc13 rely on its pairing with either of two Uevs, Uev1A or Mms2. Structurally, we demonstrate that Mms2 and Uev1A differentially modulate the length of Ubc13-mediated Lys63-linked polyubiquitin chains. Functionally, we describe that Ubc13–Mms2 is required for DNA damage repair but not nuclear factor κB (NF-κB) activation, whereas Ubc13–Uev1A is involved in NF-κB activation but not DNA repair. Our finding suggests a novel regulatory mechanism in which different Uevs direct Ubcs to diverse cellular processes through physical interaction and alternative polyubiquitination.

Introduction

Protein modification by ubiquitin (Ub) is a fundamental post-translational modification event that serves as a signaling function in diverse biological processes, including stress responses, cell cycle progression, oncogenesis, and antigen presentation (Pickart, 2001b). The ubiquitination of a protein substrate involves the formation of an isopeptide bond between a substrate lysine residue and the COOH-terminal carboxyl group of Ub Gly76. This reaction is accomplished through the sequential actions of several classes of enzymes. A Ub-activating enzyme (Uba or E1) hydrolyzes ATP and forms a high-energy thioester between a cysteine of its active site and the COOH terminus of Ub. Activated Ub is then passed on to a Ub-conjugating enzyme (Ubc or E2), which forms thioester-linked complexes with Ub in a similar fashion. Next, Ub is covalently attached to the substrate protein by a Ub ligase (E3). The lysine residues within Ub itself may also serve as substrates, leading to the formation of poly-Ub chains (Chau et al., 1989); this poly-Ub chain assembly may be facilitated by a recently identified E4 (Koegl et al., 1999).

Most organisms have only one E1 enzyme, whereas all organisms have many E2 and E3 enzymes. All the known E2s belong to a single family, containing a conserved catalytic core domain harboring the active site cysteine residue (Pickart, 2001b). On the other hand, many known E3s belong to several different protein families, including HECT, RING (Pickart, 2001a), and U-box (Hatakeyama and Nakayama, 2003). The large number of E3s is consistent with the observation that the E3 acts as the primary substrate recognition factor in the ubiquitination reaction, whereas the E2 is thought to be involved in the reaction largely through its association with a given E3.

Poly-Ub chains attached to a substrate can also be linked through different lysines within Ub, and it has become clear that the signaling properties of ubiquitination depend on the topology of poly-Ub chains. For example, it has been well established that poly-Ub chains linked through Lys48 are the principal signal to target a substrate for proteolysis by 26S proteasomes, whereas Lys63-linked chains play a regulatory

P.L. Andersen and H. Zhou contributed equally to this paper.

Correspondence to Wei Xiao: wei.xiao@usask.ca

Abbreviations used in this paper: CPT, camptothecin; DSB, double-stranded break; ICC, immunocytochemistry; LPS, lipopolysaccharide; MMS, methyl methanesulfonate; PCNA, proliferating cell nuclear antigen; PRR, postreplication repair; RNAi, RNA interference; siRNA, small interference RNA; Ub, ubiquitin.

The online version of this article contains supplemental material.

The Journal of Cell Biology, Vol. 170, No. 5, August 29, 2005 745–755
http://www.jcb.org/cgi/doi/10.1083/jcb.200502113

Supplemental Material can be found at:
http://www.jcb.org/cgi/content/full/jcb.200502113/DC1

role in diverse signaling pathways in a nonproteolytic fashion (Pickart, 2001b). The molecular basis for determining such specificity in chain assembly and recognition, however, remains poorly understood. So far only one E2, Ubc13, has been shown to mediate the assembly of Lys63-linked poly-Ub chains, and this activity requires a Ubc variant (Uev) as a cofactor; neither Ubc13 nor Uev alone is able to promote Lys63 poly-Ub chains (Hofmann and Pickart, 1999; McKenna et al., 2001). Uev is defined as a protein that resembles Ubc in structure and amino acid sequence, but does not contain a cysteine residue in the presumptive active site, rendering the protein catalytically inactive (Broomfield et al., 1998; Sancho et al., 1998). The prototype Uev, Mms2, was first isolated and characterized from the budding yeast *Saccharomyces cerevisiae* and is required for error-free postreplication repair (PRR; Broomfield et al., 1998). The crystal structure (Moraes et al., 2001; VanDemark et al., 2001) and NMR analysis (McKenna et al., 2001) of the Ubc13–Mms2 heterodimer show that Mms2 binds the acceptor Ub in an orientation that allows only Lys63, and not Lys48, to approach the active site on Ubc13. Subsequent studies indicate that many other proteins contain Uev domains. Collectively called the Uev family of proteins, they are as ancient as the Ubc family of proteins (Villalobo et al., 2002) and they are highly conserved in the eukaryotic kingdom, from protists to human (Brown et al., 2002). Higher eukaryotes, including plants and mammals, contain an increasing number of Uev proteins (Wong et al., 2003), suggesting that the Uev family of proteins may have evolved to increase diversity and selectivity in Ub conjugation. Nevertheless, it remains unknown whether these evolved Uev proteins are functionally redundant or each plays a specific role in discrete cellular processes. We addressed this question in the current study and found that Mms2 and Uev1, two mammalian homologues of the yeast Mms2, although sharing >90% amino acid sequence identity to each other in their core domain (Fig. 1) and both capable of cooperating with Ubc13 to promote ubiquitination in vitro, are involved in distinct biological activities in vivo. Specifically, we demonstrated that Mms2 is required in Ubc13-dependent DNA damage response but not NF-κB activation, whereas Uev1A is involved in Ubc13-dependent NF-κB activation but not DNA damage response. Thus, our study provides novel insight that Uev family proteins may have evolved to differentially regulate E2 functions in diverse cellular processes.

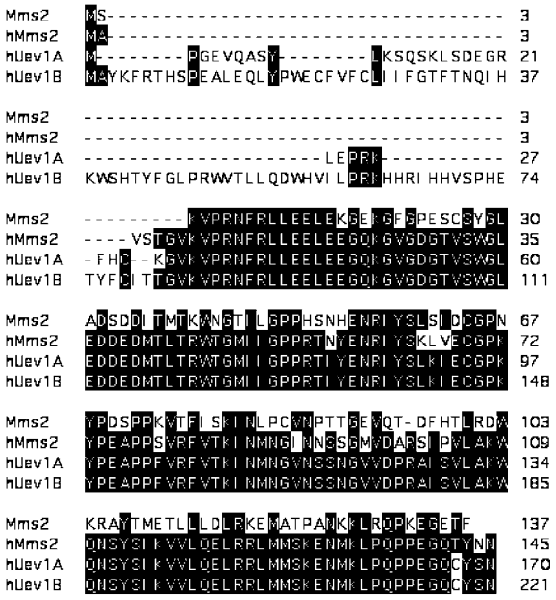

Figure 1. **Amino acid sequence comparison of yeast Mms2 and its human homologues.** The amino acid sequences are obtained from the following sources: Mms2 (Broomfield et al., 1998); hMms2 (Xiao et al., 1998); Uev1A and Uev1B (Rothofsky and Lin, 1997). The corrected Uev1A sequence as reported previously (Deng et al., 2000) was used for alignment.

Results

Rationale and hypothesis

The central hypothesis to be tested in this study is that mammalian cells have distinct responses to genotoxic and nongenotoxic stresses, which are at least partially achieved by modulation of Ubc activity through different Uevs. In particular, we propose that Mms2 and Uev1 modulate Ubc13 activity via physical interaction and recruitment of the distinct Ubc–Uev complexes into different cellular processes. Yeast Mms2 is required for an error-free mode of PRR to prevent spontaneous and damage-induced mutagenesis and genome instability. It is now clear that the yeast Ubc13–Mms2 complex targets proliferating cell nuclear antigen (PCNA) for Lys63 chain assembly (Hoege et al., 2002). In mammalian cells, a Ubc13–Uev complex was found to be involved in TRAF6-mediated regulation of IκB kinase (Deng et al., 2000) and Bcl10/MALT-mediated Lys63-linked polyubiquitination of NEMO/IKKγ (Zhou et al., 2004), both leading to NF-κB activation. Hence, these two pathways and additional activities related to these pathways were examined in the context of Ubc13 and Uev requirements.

Ubc13–Uev complex formation

A prerequisite for our hypothesis is that both Mms2 and Uev1 form stable complexes with Ubc13. Although the physical interaction between Ubc13 and Uev has been reported in various studies (Deng et al., 2000; Hofmann and Pickart, 1999; McKenna et al., 2001), we decided to systematically test all three Mms2 homologues found in human cells for their in vitro and in vivo (in yeast cells) interactions. As shown in Fig. 2 A, bacterial cell extracts from cells expressing GST-Mms2 (lane 2) and GST-Uev1A (lane 3) were able to pull down purified recombinant Ubc13 by GST affinity. In contrast, extracts from cells expressing GST alone (not depicted) or GST-Uev1B (Fig. 2 A, lane 4) were unable to pull down detectable amounts of Ubc13. To further confirm the in vitro data, yeast two-hybrid analysis was performed by fusing Uev with the Gal4 DNA binding domain ($Gal4_{BD}$) at the COOH terminus and Ubc13 with the Gal4 activation domain ($Gal4_{AD}$) at the NH_2 terminus. As shown in Fig. 2 B, only Mms2-$Gal4_{BD}$ and Uev1A-$Gal4_{BD}$ were able to interact with $Gal4_{AD}$-Ubc13, resulting in simultaneous activation of P_{GAL1}-HIS3 and P_{GAL2}-ADE2, whereas Uev1B-$Gal4_{BD}$ was unable to interact with $Gal4_{AD}$-Ubc13. To determine whether the human Ubc13–Uev interaction is related to its biological functions in yeast cells, we attempted to functionally

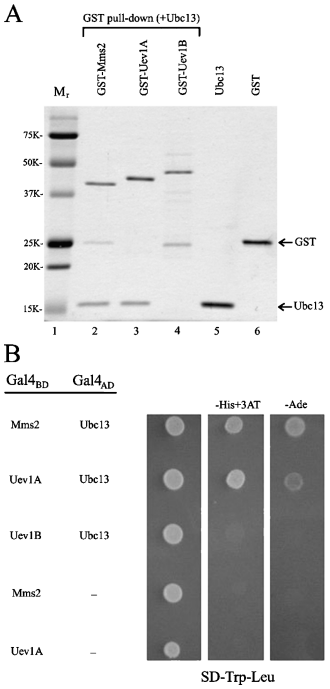

Figure 2. **Ubc13–Uev complex formation.** (A) In vitro GST pull-down assay. BL21(DE3)-RIL cells transformed with pGEX-hMMS2, pGEX-UEV1A, and pGEX-UEV1B were grown and target gene expression was induced by adding IPTG. Crude cell extracts were used to load GST affinity MicroSpin columns and 40 μg of purified hUbc13 was later added. The resulting elution was loaded onto an SDS-PAGE gel and stained with Coomassie blue. Components used in each sample are indicated on the top. Lane 5 contains 1 μg of purified hUbc13 and lane 6 contains 1 μg of purified GST, as indicated by arrows. (B) Yeast two-hybrid analysis of Ubc13–Uev interactions. Cotransformed plasmids are indicated on the left. The plates were incubated for 3 d before taking the photograph. Only one representative transformant from each combination is shown. Cells cotransformed with pUev1B-G4BD/pGAD424 and pG4BD-1/pGAD-Ubc13 were also negative (not depicted).

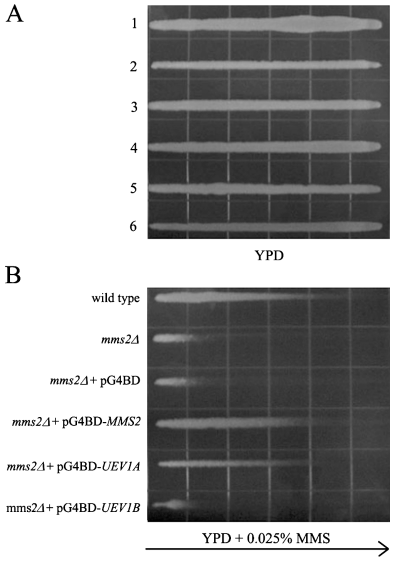

Figure 3. **Heterologous function of human *UEV* genes in yeast.** WXY903 (*mms2Δ::HIS3*) was transformed with various pUev-G4BD plasmids and the transformants were compared with HK580-10D (wild type) in a gradient plate assay for their ability to complement the yeast *mms2* defect. Overnight cell cultures were printed on YPD (A) or YPD + 0.025% MMS (B) plates and incubated for 36 h before taking the photograph. The arrow points toward higher MMS concentration.

complement the yeast *mms2* null mutant by expressing each of the Uev-Gal4$_{BD}$ constructs. Although expression of Mms2-Gal4$_{BD}$ and Uev1A-Gal4$_{BD}$ was able to fully alleviate the severe methyl methanesulfonate (MMS) sensitivity of *mms2* cells to the wild-type level in a gradient plate assay, vector alone or the Uev1B-Gal4$_{BD}$ construct failed to rescue *mms2*-deficient cells from killing by MMS (Fig. 3). The lack of Uev1B activity in yeast cells is likely due to the extended NH_2-terminal sequence, as deletion of the NH_2-terminal 80–amino acid coding region from *UEV1B* restores its DNA repair function in yeast (Xiao et al., 1998) and the interaction with Ubc13 in a yeast two-hybrid assay (unpublished data). Due to the lack of detection of Uev1B–Ubc13 interaction, and our previous observation (Franko et al., 2001) that mouse cells do not express the corresponding *Uev1B* transcript, we decided to focus our attention on the cellular functions of Mms2 and Uev1A in this study.

Ubc13 and Mms2, but not Uev1A, are involved in DNA damage response

To investigate the involvement of Ubc13 and Uevs in DNA repair, we examined nuclear foci formation in response to DNA damage. After DNA damage, many repair enzymes form stable focal localizations near sites of DNA damage, depending on the extent and type of damage. In particular, both Rad51 and Mre11/Rad50/Nbs1 form DNA damage–induced nuclear foci, but their distribution patterns are different (Maser et al., 2001), which probably reflects their involvement in distinct recombination processes. We exposed NIH 3T3 and HepG2 cells to various doses of DNA damaging agents such as MMS, UV, and camptothecin (CPT), among which CPT treatment appears to generate the most significant effect. CPT is a topoisomerase I inhibitor, which converts a single-stranded DNA break into a double-stranded break (DSB) at the replication fork (Ryan et al., 1991; Tsao et al., 1993). Hence, CPT treatment serves as a highly specific and predictable cause of DNA lesions.

Because Ubc13 and Uev are thought to be freely diffusible between the cytoplasm and the nucleus, we attempted to refine their localization by using an in situ cell fractionation procedure before fixation, which is a method frequently applied to identify nuclear localization of DNA repair proteins (Andegeko et al., 2001). After CPT treatment, nuclear foci positive for Mre11 (Fig. 4 A), Rad51 (Fig. 4 B), and Ubc13 (Fig. 4, A and B) immunoreactivity were observed after detergent extraction under a stringent condition capable of releasing the diffuse Ubc13 nuclear staining in the S phase cells (not depicted). Surprisingly, CPT-induced Ubc13 nuclear foci exhibit morphological distributions distinct from both Rad51 and Mre11 foci. It was found that within 1 h after CPT treatment, Rad51 and Mre11 foci become very apparent in a significant number of cells as fine nuclear foci; however, Ubc13 foci were not apparent until nearly 4 h after CPT treatment. A time course analysis indicates that as time progressed nearly all the cells retained Ubc13 immunoreactivity (Fig. S1, available at http://www.jcb.org/cgi/content/full/jcb.200502113/DC1). Furthermore, Ubc13 foci appeared as

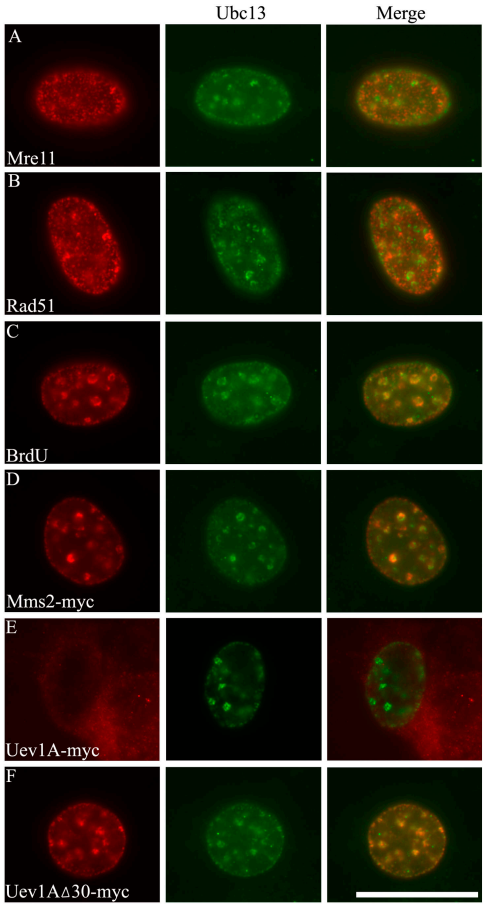

Figure 4. **CPT-induced nuclear foci formation.** ICC of 3T3 cells after CPT treatment (5 μM for 4 h) and in situ cell fractionation reveals Ubc13 nuclear foci (4E11 as primary antibody and Alexa488 as secondary antibody). These foci are compared, by merging images, with those of Mre11 (A), Rad51 (B), and BrdU (C) and in 3T3 cells transfected with Mms2-myc (D), Uev1A-myc (E), and Uev1AΔ30-myc (F) viewed by using specific primary antibodies and the Alexa546 secondary antibody, except in C, in which Alexa546 is directly conjugated with anti-BrdU. Bar, 5 μm.

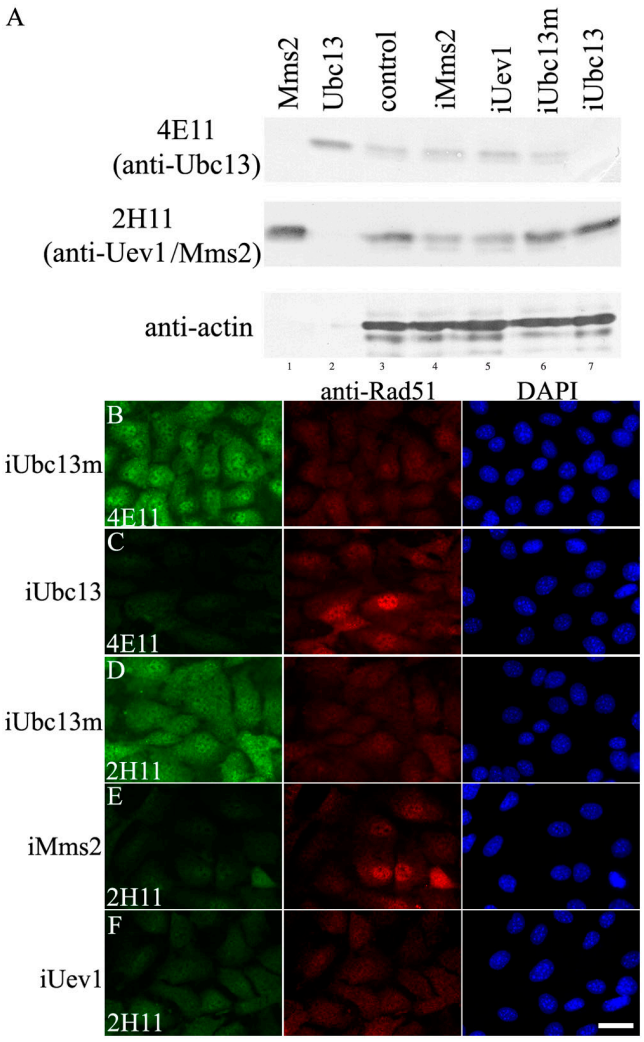

Figure 5. **Spontaneous Rad51 nuclear foci formation after RNAi treatment.** (A) Western blot analysis of purified recombinant hMms2 (lane 1), hUbc13 (lane 2), and 3T3 total cell extracts (lanes 3–7) using 4E11 (anti-Ubc13) or 2H11 (anti-hMms2) as primary antibodies. Lanes 4–7 represent cultures transfected with various RNAi constructs as indicated. Note that 2H11 (and other anti-hMms2 mAbs) detected only one band from mammalian cell extracts, which corresponds to the migration of Mms2, but was found to contain both Mms2 and Uev1A by mass spectrometry (not depicted). (B–F) 4 d after transfection of 3T3 cells with the indicated RNAi constructs against specific target genes, cells were stained with either 4E11 (B and C) or 2H11 (D–F) plus Alexa488 to reveal Ubc13 and Uev immunoreactivity, respectively. The same cells were also stained with anti-Rad51 plus Alexa546 to reveal Rad51 nuclear foci and with DAPI to reveal nuclei of all cells. Bar, 10 μm.

punctuate structures distinctly larger than the fine granular foci of either Rad51 or Mre11 and were colocalized with those of BrdU incorporation (Fig. 4 C), implying that Ubc13 is involved in DNA synthesis under DNA damage conditions. The punctuate pattern of Ubc13 foci and BrdU incorporation agrees with a previous finding (Sakamoto et al., 2001) that Rad51 nuclear foci are distinct from the distribution pattern of BrdU incorporation after CPT treatment.

Because mAbs raised against human Mms2 were unable to distinguish Mms2 from Uev1, we studied their subcellular localization by expressing either myc-tagged Mms2 or Uev1A in 3T3 and HepG2 cells. Immunofluorescence study using mAb 9E10 against c-myc showed that Mms2 and Uev1 were distributed in both nucleus and cytoplasm regardless of DNA damage treatment (Fig. S2, available at http://www.jcb.org/cgi/content/full/jcb.200502113/DC1). However, after CPT treatment and detergent extraction, nuclear foci containing Mms2-myc were observed, and they were colocalized with endogenous Ubc13 foci (Fig. 4 D). In contrast, Uev1A-myc was not found in the nuclear foci of CPT-treated cells and cannot be colocalized with those of Ubc13 (Fig. 4 E). These observations provide strong evidence that the Ubc13–Mms2 complex is involved in DNA damage repair, which is distinct from the Ubc13–Uev1A complex.

Suppression of Ubc13 or Mms2 results in an increase in Rad51 foci formation

To further address whether the Ubc13–Mms2 and Ubc13–Uev1A complexes play a role in protecting mammalian cells from genomic instability under normal growth conditions, we attempted to experimentally suppress target gene expression by

Table I. **Percentage of Rad51 nuclear foci–positive cells after RNAi treatment**

RNAi	Total cells counted	Rad51-positive nuclei	SD	P with respect to control
		%		
Ubc13m	1,010	8	± 1.3	–
Ubc13	991	33	± 2.5	< 0.001
Mms2	970	32	± 2.5	< 0.001
Uev1A	1,011	8	± 1.7	1.0

an RNA interference (RNAi) technology (Yu et al., 2002) and examine its effects on endogenous DNA damage, as measured by spontaneous Rad51 and Mre11 nuclear foci formation. The effects of this method were examined by Western blot analysis using Ubc13 and Mms2/Uev1-specific mAbs. As shown in Fig. 5 A, transfection of mouse 3T3 cells with RNAi against Ubc13 (iUbc13) reduced target Ubc13 to an undetectable level (lane 7) with no effect on Mms2/Uev1A expression. This suppression is highly specific, as a single nucleotide mismatch (iUbc13m) completely abolished the target gene suppression (Fig. 5 A, lane 6). Transfection with iMms2 (Fig. 5 A, lane 4) or iUev1 (lane 5) resulted in partial reduction of 2H11 immunoreactivity; the remaining immunoreactivity is presumably due to cross-reaction of 2H11 to both Mms2 and Uev1. Similar results were also obtained by immunocytochemical analysis (Fig. 5, D–F), which together demonstrate that, like iUbc13, the suppression of target genes by iMms2 and iUev1 was also highly efficient and specific. Experimental ablation of either Ubc13 or Mms2 in 3T3 cells was accompanied by an increased number of cells exhibiting Rad51 nuclear foci from a basal level of ~8 to 33 and 32%, respectively; the difference is consistent in three independent experiments and statistically significant ($P < 0.001$; Fig. 5, C and E; and Table I). In contrast, cells transfected with iUbc13m (Fig. 5, B and D) did not affect Rad51 foci formation, suggesting that the induced Rad51 nuclear foci were indeed due to the increased spontaneous DNA damage when Ubc13 or Mms2 activity was compromised. As expected, iUev1 transfection did not result in an increased number of cells containing Rad51 nuclear foci (Fig. 5 F and Table I), suggesting that Uev1 is not involved in DNA damage avoidance. It was noted that within the experimental period, cell viability, doubling time, and the percentage of Mre11-positive nuclei were not altered in any of the aforementioned RNAi transfectants (unpublished data). Thus, we conclude from the aforementioned observations that Ubc13 and Mms2 are required to prevent endogenous DNA damage and double strand break formation, whereas Uev1 is not involved in this process. To our knowledge, this is the first experimental evidence that a mammalian Ubc13–Uev complex protects cells from spontaneous DNA damage.

Suppression of Ubc13 or Uev1 reduces TRAF2- and TRAF6-mediated NF-κB activation

The TNF associated factors 2 and 6 (TRAF2 and TRAF6) are involved in the signaling cascades initiated by TNF receptors, Toll-like receptors, and several interleukin receptors (Sun and

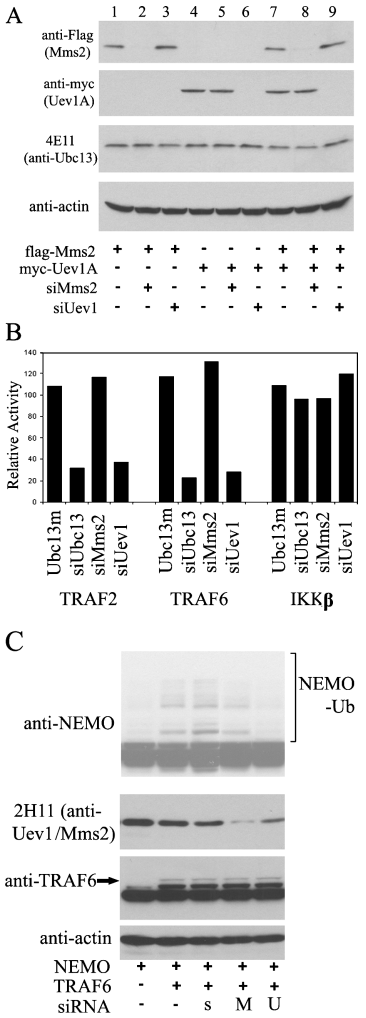

Figure 6. **Ablation of Uev1A suppresses TRAF-induced NF-κB activity and NEMO polyubiquitination in 293T cells.** (A) Western blot analysis confirms RNAi specificity and efficacy of target suppression. (B) Modulation of IKKβ-, TRAF2-, and TRAF6-induced NF-κB activity by ablation of Ubc13, Uev1, or Mms2. The relative NF-κB activity was calculated against transfected cells without siRNA treatment. (C) Effects of Mms2 or Uev1 ablation by siRNA on NEMO polyubiquitination. s, scrambled nonspecific siRNA; M, siMms2; U, siUev1. The arrow points to TRAF6.

Chen, 2004). Both TRAF2 (Shi and Kehrl, 2003) and TRAF6 (Deng et al., 2000) have been implicated as E3s for Ubc13-mediated NF-κB activation; however, it remains unclear which Uev is required for Ubc13 function in these signaling pathways. To address this issue, we used synthetic small interference RNA (siRNA) to specifically inhibit the expression of either Mms2 or Uev1. Because 2H11 monoclonal antibody recognizes both Mms2 and Uev1, we verified the specificity of our targeting siRNAs for either Mms2 or Uev1 by examining their effects in knocking down the expressions of FLAG-Mms2 and/or myc-Uev1A. As shown in Fig. 6 A, siRNA against Mms2 (lanes 2 and 8) or Uev1 (lanes 6 and 9) specifically inhibits its target gene expression but does not display a cross inhibitory effect. Consistent with our previous findings (Zhou et al., 2004), siRNA-targeting Ubc13 significantly reduced TRAF2- and TRAF6-stimulated NF-κB activation (Fig. 6 B). Moreover,

siRNA-targeting Uev1 but not Mms2 inhibited TRAF2- and TRAF6-stimulated NF-κB activation. This effect is apparently specific for TRAF2- and TRAF6-dependent ubiquitination to activate NF-κB because neither Ubc13 nor Uev1 silencing affected IKKβ-mediated NF-κB activation (Fig. 6 B). These results highlight a specific role for Uev1 but not Mms2 in cooperating with Ubc13 in activating the NF-κB pathway.

We have previously established that NEMO/IKKγ is a cellular target of Lys63 polyubiquitination and that siRNA suppression of Ubc13 abolishes NEMO polyubiquitination (Zhou et al., 2004). To determine whether a Uev is required for NEMO polyubiquitination and, more importantly, which Uev plays such a role, we experimentally suppressed either Mms2 or Uev1 in HEK 293T cells by siRNA treatment and monitored NEMO ubiquitination. As shown in Fig. 6 C, cells treated with siRNA-targeting Uev1 (fifth lane) significantly reduced NEMO ubiquitination. In contrast, suppression of Mms2 (Fig. 6 C, fourth lane) did not appear to have a significant effect on NEMO ubiquitination compared with untreated or random siRNA-treated cells. Due to the cross immunoreactivity of 2H11 to both Mms2 and Uev1, we were unable to quantitatively determine the efficacy of siRNA treatment in this experiment, although siRNA against Mms2 or Uev1 variably reduced 2H11 immunoreactivity. Nevertheless, the result is consistent with that of the NF-κB activity assay (Fig. 6 B) indicating that only Uev1A, but not Mms2, is involved in the NF-κB activation via Lys63-linked polyubiquitination of NEMO.

Ubc13 and Uev1 are required for lipopolysaccharide (LPS)-induced NF-κB activation

The bacterial endotoxin LPS stimulates NF-κB activation in microglia (Bonaiuto et al., 1997). To determine the physiological significance of the Ubc13–Uev complex in this pathway, we monitored the nuclear translocation of the p65 subunit of NF-κB in response to LPS in primary murine microglia cells. In untreated cells, p65 resided mainly in the cytoplasm, whereas upon LPS treatment, p65 rapidly translocated into the nucleus (unpublished data). As shown in Fig. 7, RNAi directed to reduce Mms2 did not affect p65 translocation to the nucleus after LPS treatment. However, after LPS treatment, the number of microglia nuclei containing significant p65 immunoreactivity was reduced from nearly 100% to ∼30% in cells transfected with RNAi constructs directed to reduce either Ubc13 or Uev1. This result indicates that the activities of Ubc13 and Uev1A, but not Mms2, are indeed required in the NF-κB signaling pathway.

Distinct Lys63 chain assembly activities between Mms2 and Uev1A

Given that both Uev1A and Mms2 are able to form a stable complex with Ubc13 in vivo and in vitro, but their biological functions are distinct, we hypothesize that the structural and sequence differences between Uev1A and Mms2 are responsible for their distinct intracellular signaling pathways. As the first step toward understanding how Uev1A and Mms2 are involved in distinct cellular processes, we performed an in vitro polyubiquitination activity assay using highly purified components. To prevent E2 self-ubiquitination, a Ubc13 derivative (Ubc13K92R) was used in the assay in combination with either Mms2 or Uev1A. We have previously shown that both Ubc13 and Ubc13K92R were able to form di-Ub conjugates with equal efficiency (McKenna et al., 2001); however, neither (Fig. 8, lanes 1 and 2) is able to carry out Ub chain assembly in the absence of Uev. The addition of Mms2 could only support di-Ub formation (Fig. 8, lane 3), in contrast to the poly-Ub formation in the presence of Uev1A (Fig. 8, lane 5). Uev1A differs from Mms2 in two aspects, namely, the nonconserved NH_2-terminal 30 amino acids and <10% sequence variation in the remaining core domain (Fig. 1). To determine which difference is responsible for the observed poly-Ub versus di-Ub formation, a 30-residue truncation was made in Uev1A such that it resembled the core region of Mms2. Incubating Uev1AΔ30 with Ubc13K92R resulted in only di-Ub formation (Fig. 8, lane 4) in a manner similar to that observed with the addition of Mms2. These observations suggest that the additional NH_2-terminal region of Uev1A is responsible for Ubc13-mediated poly-Ub chain assembly through Lys63-Gly76 linkage in vitro and that the differential polyubiquitination activity between Uev1A and Mms2 may play a role in their distinct cellular functions.

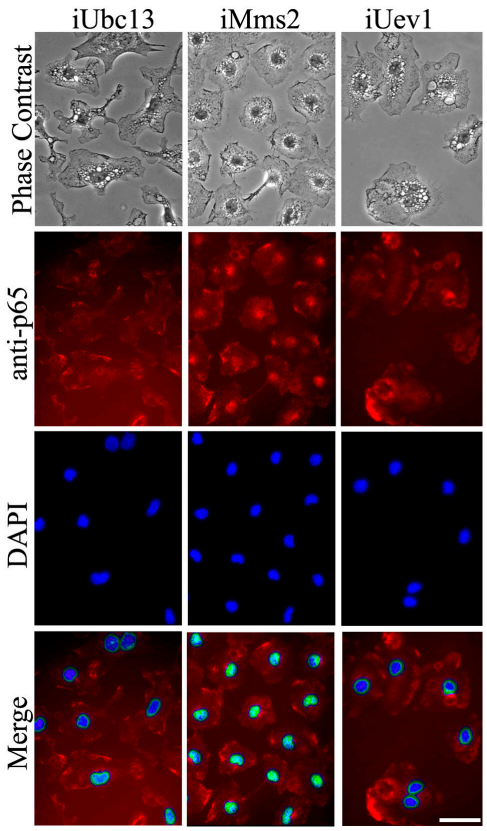

Figure 7. **Requirement of Ubc13 and Uev1A for LPS-induced p65 translocation.** Phase contrast, p65-ICC, and DAPI staining were performed 4 d after transfection of mouse microglia with RNAi constructs as indicated, followed by a 1.5-h exposure to 1 μg/ml LPS and fixation. Merged images indicate colocalization of p65 immunostaining with nuclei. Identical color adjustment was made to all merged images to enhance differential colocalization. Bar, 10 μm.

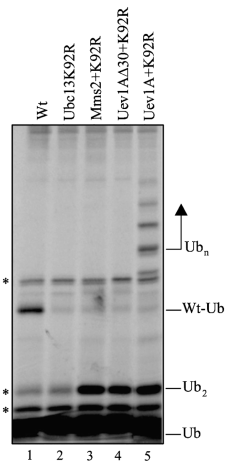

Figure 8. **Ub chain building.** Mms2 and Uev1A were assayed for Ub chain building activity using an in vitro ubiquitination reaction. The components of the reaction are noted in Materials and methods. The concentration of wild-type hUbc13 (Wt), hUbc13K92R (K92R), hMms2, Uev1A, and Uev1AΔ30 is 250 nM. The positions of free Ub (Ub), di-Ub (Ub_2), Ubc13-Ub (Wt-Ub), and multi-Ub chains (Ub_n) are indicated. Major contaminant bands from the ^{35}S-Ub preparation, including the background band comigrating with Ub_2, are indicated by an asterisk.

To address whether the NH_2-terminal extension of Uev1A dictates its cellular activity, we made a corresponding Uev1AΔ30-myc construct, used it to transiently transfect mouse 3T3 cells, and analyzed Uev1AΔ30-myc cellular localization as previously described. Compared with Uev1A-myc, Uev1AΔ30-myc did not appear to affect cellular distribution before or after CPT treatment (Fig. S2, C and C′); however, after detergent extraction, Uev1AΔ30-myc was found in the nuclear foci and colocalized with Ubc13 (Fig. 4 F), which is reminiscent of Mms2-myc (Fig. 4 D). Hence, the Uev1A core domain behaves like Mms2 rather than the full-length Uev1A, indicating that the NH_2-terminal extension of Uev1A is probably a determinant of distinct Uev functions in vivo.

Discussion

Cells are facing two rather different types of environmental or even endogenous stresses. Genotoxic stress threatens genome stability, evokes cell cycle arrest, and induces DNA repair capacity, whereas cellular responses to nongenotoxic stresses would be primarily to enhance cell survival and proliferation. Covalent modification of target proteins by Ub and Ub-like proteins is primarily involved in stress responses. It has been reported recently that Ubc13 and its cognate Lys63 chain assembly is required for two important stress responses, namely DNA repair and NF-κB activation. It is unclear, however, how Ubc13 is involved in these two seemingly contradictory pathways, as error-free PRR in yeast prevents spontaneous and DNA damage–induced mutagenesis (Broomfield et al., 1998) and a similar role in mammals would protect cells from carcinogenesis. In contrast, activation of NF-κB has been described as a primary prosurvival and antiapoptotic response and its activity has been linked to various cancers (Dixit and Mak, 2002). Is the error-free PRR pathway conserved in mammals? If it is, how do mammalian cells regulate the two opposite pathways? The discovery of two yeast *MMS2* homologues in human cells, *hMMS2* and *UEV1* (Xiao et al., 1998), provides a key to solve the paradox; however, the sequence alignment and studies to date do not provide adequate information as to which Uev is involved in which pathway. The situation becomes even more complicated by the observation that expression of either *hMMS2* or *UEV1* is able to rescue the yeast *mms2* mutant from killing by DNA damage, and that both Mms2 and Uev1 are able to support Lys63 polyubiquitination in vitro leading to NF-κB activation (Deng et al., 2000; Zhou et al., 2004). Here, we provide evidence that different Ubc13 activities are modulated by the two Uevs that act as regulatory subunits for Lys63-mediated target modification. This discovery may reveal a novel regulatory mechanism for stress response.

Mms2 and DNA repair

Lower eukaryotes such as budding and fission yeasts contain a single Ubc13 and its Uev partner, Mms2, which is essential for error-free PRR (Broomfield et al., 1998; Brusky et al., 2000; Brown et al., 2002). The Ubc13–Mms2 activity in yeast results in polyubiquitination of PCNA after its monoubiquitination at the Lys164 residue by the Rad6–Rad18 complex (Hoege et al., 2002); PCNA modified by Lys63-linked poly-Ub chain probably acts to switch a mode of damage tolerance from translesion DNA synthesis and genome instability mediated by mutagenic DNA polymerases (Stelter and Ulrich, 2003; Haracska et al., 2004) into an error-free PRR via sister chromatid exchange and/or template switching (Pastushok and Xiao, 2004). We demonstrate that the Ubc13–Mms2 complex in mammalian cells probably inherits the same activity. First, upon DNA damage, Ubc13 and Mms2 form nuclear foci with newly synthesized DNA, suggesting that this complex resides at or near the replication fork. Second, ablation of either Ubc13 or Mms2 results in increased spontaneous DNA strand breaks that induce Rad51 nuclear foci formation. Third, Mms2 and Ubc13 are retained in the S phase nucleus and colocalized with PCNA (unpublished data). Finally, we also observed that suppression of either Ubc13 or Mms2 results in slightly but significantly increased sensitivity to killing by DNA damaging agents and that the effect appears to be synergistic with simultaneous suppression of Rev3 (unpublished data), which is reminiscent of the corresponding yeast mutant phenotypes (Broomfield et al., 1998) and agrees with our previous observations (Li et al., 2002) that antisense suppression of *hMMS2* results in phenotypes characteristic of error-free PRR defects. In contrast, RNAi suppression of *UEV1* does not share the aforementioned phenotypes, nor is it found in S phase or damage-induced nuclear foci. Hence, Uev1 is not involved in DNA repair.

In summary, we found that *UBC13* and *MMS2* not only protect mammalian cells from genome instability caused by environmental DNA damage but probably also prevent spontaneous DNA damage or replication fork collapse. When *UBC13* or *MMS2* expression is compromised, cells probably accumulate DSBs that in turn induce Rad51 nuclear foci formation. Our observation that RNAi suppression of *UBC13* and *MMS2* only induces Rad51 foci, but not Mre11 foci, indicates that DSBs accumulated due to lack of Ubc13–Mms2 signaling would have to be repaired by homologous recombination instead of nonhomologous end joining, which is consistent with a previous observation that suppression of *hMMS2* completely abolishes UV-induced gene conversion (Li et al., 2002).

Uev1 and NF-κB activation

Before this study, it was unclear which Uev is involved in TRAF2- and TRAF6-mediated NF-κB activation because both Mms2 and Uev1A are able to mediate the activity in vitro. Our genetic analysis clearly demonstrates that it is Ubc13 and Uev1, but not Mms2, that are required for TRAF2- and TRAF6-mediated NF-κB activation, and that this activity is in a step upstream of IKK but downstream or together with TRAF2 and TRAF6. We further demonstrate that Uev1, but not Mms2, is required for TRAF6-induced NEMO polyubiquitination. This conclusion fits well with our previous observation that NEMO serves as the Lys63 chain target (Zhou et al., 2004) and supports a recently proposed model (Sun et al., 2004) in which the MALT1 oligomers bind to TRAF6, induce TRAF6 oligomerization, and activate the E3 activity of TRAF6 to polyubiquitinate NEMO in the presence of Ubc13–Uev.

NF-κB activation has been described as a prosurvival and antiapoptotic response to bacterial and viral infections and other environmental stresses. To address the physiological relevance of Ubc13–Uev1 in stress response, we show that LPS-induced NF-κB activation in primary microglia cells requires both Ubc13 and Uev1, but not Mms2. Constitutive activation of NF-κB is linked to cancers such as lymphoma and other human diseases (Dixit and Mak, 2002). Interestingly, human *UEV1* has been independently isolated by its ability to transactivate the *c-fos* promoter (Rothofsky and Lin, 1997), and its transcript level increases when SV40-transformed human embryonic kidney cells undergo immortalization (Ma et al., 1998) and decreases upon differentiation of the human colon carcinoma cell line HT-29-M6 (Sancho et al., 1998). Furthermore, the *UEV1* mRNA level is elevated in all human tumor cell lines examined compared with normal tissues (Xiao et al., 1998), and the gene is located to chromosome 20q13.2, a region where gene amplification is frequently observed in breast cancer (Kallioniemi et al., 1994; Tanner et al., 1994; Brinkmann et al., 1996) and other tumors (El-Rifai et al., 1998), as well as in virus-transformed immortal cells (Savelieva et al., 1997). These observations collectively place *UEV1* as a candidate protooncogene. Indeed, we find that experimental overexpression of *UEV1A* is sufficient to activate NF-κB and inhibit apoptosis (unpublished data). Conversely, the tumor suppressor gene product CYLD appears to be a Lys63-specific deubiquitination enzyme responsible for the removal of Ub from NEMO (Brummelkamp et al., 2003; Kovalenko et al., 2003). Hence, Uev1 serves as a regulatory subunit for Ubc13-mediated Lys63 chain assembly and may be an excellent target for cancer therapy.

Mms2 versus Uev1A: a novel regulatory mechanism?

Protein ubiquitination and its related processes have been unveiled as a versatile mechanism to regulate protein activities in eukaryotes. Our data present a previously undescribed mechanism by which different Uev molecules act as mutually exclusive regulatory subunits of an E2 (Ubc13) to different subcellular locations and/or to modify different target proteins. Although Uev1A is required for NEMO polyubiquitination in the cytoplasm, mammalian Mms2, if it behaves like its yeast homologue, may be involved in the ubiquitination of PCNA in the nucleus.

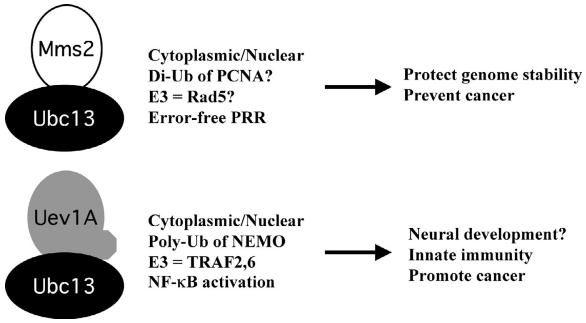

Figure 9. **A working model of Ubc13–Uev functions in human cells.** This model is based on data and discussion presented in this paper as well as some previous papers. Please note that a mammalian Rad5 homologue has not been identified.

Sensing and repairing DNA damage and NF-κB activation are two rather distinct cellular processes and lead to opposite cellular consequences. The former will arrest cell cycle progress until DNA synthesis is complete or, if the damage is too severe to repair, cause apoptosis, whereas the latter will promote cell survival and prevent apoptosis. How do cells sense these different stresses and respond correctly? Our findings suggest that the two highly conserved but functionally distinct Uevs may play a central role in this decision-making process. Three alternative, but not mutually exclusive, mechanisms may be envisioned to achieve such regulation. First, Uev1A and Mms2 may compete for binding to limited Ubc13 in the cell. It is interesting to notice that structural analyses (McKenna et al., 2001; Moraes et al., 2001; VanDemark et al., 2001) have shown that the Ubc13–Uev heterodimer formation is in a 1:1 ratio, that the binding affinity of Ubc13 for Mms2 and Uev1A is comparable (McKenna et al., 2003), and that Mms2 and Uev1A are distributed in both the cytoplasm and the nucleus. Hence, Uev1A can readily compete with Mms2 to prevent it from forming a complex with Ubc13 in the nucleus. The fact that Uev1A is found in the nucleus with no defined role described thus far suggests that perhaps Uev1A competes with Mms2 in the nucleus for binding to Ubc13 and acts as an antagonistic factor. This possibility is particularly attractive because it would also explain its oncogenic property, as inhibition of error-free PRR in yeast cells results in a massive increase in spontaneous mutagenesis (Broomfield et al., 1998), which would lead to genome instability and tumorigenesis in mammals. Second, cellular Ubc13 may not be limited; however, it is not activated until binding to a cognate Uev. This hypothesis predicts that Mms2 and Uev1A are differentially activated depending on source of stress (e.g., genotoxic vs. nongenotoxic), and that the activated Ubc13–Uev complex determines pathway specificity by either associating with a specific E3 or other cellular components. The third possible mechanism is that Mms2 and Uev1 selectively activate target proteins through di- and polyubiquitination, respectively, as demonstrated in this study. We have demonstrated that NEMO is polyubiquitinated by Ubc13–Uev1A in vivo. In contrast, despite repeated studies on monoubiquitinated PCNA (Kannouche

et al., 2004; Watanabe et al., 2004), it is not yet known whether PCNA is di- or polyubiquitinated in vivo or in vitro. Nevertheless, we are able to show that the NH_2-terminal extension of Uev1A is probably the determinant of functional specificity and that the core domain of Uev appears to play a default function in DNA repair.

In summary, we demonstrate that Ubc13-mediated ubiquitination can coordinate cellular responses to both DNA damage as well as nongenotoxic stresses; its target selection and mode of response (e.g., DNA repair or cell proliferation) is determined not only by E3 proteins but also by a Uev as its regulatory subunit. Hence, we propose that the Uevs serve as an essential modulator of E2 ubiquitination activity. A working model based on the aforementioned analyses is depicted in Fig. 9. It should be noted that the aforementioned possibilities are not mutually exclusive. For example, Uev1A can recruit Ubc13 to a process that directly promotes tumorigenesis and meanwhile prevent Ubc13–Mms2-mediated error-free DNA repair.

Conventional selectivity of Ub addition is thought to be under the direct influence of E3 enzymes, which target specific substrates. Here, we describe a novel mechanism that regulates the type and length of Ub chains and potentially the target proteins. Given recent reports that Lys63 chains are involved in diverse functions, such as DNA repair (Broomfield et al., 1998), stress response and immunity (Deng et al., 2000; Wang et al., 2001; Zhou et al., 2004), neurodegeneration (Doss-Pepe et al., 2005; Lim et al., 2005), ribosomal activity (Spence et al., 2000), endocytosis (Galan and Haguenauer-Tsapis, 1997), that some of them do require Ubc13–Uev (Bothos et al., 2003; Doss-Pepe et al., 2005), and that additional Uev proteins have been identified with known or unknown activities (Wong et al., 2003), our findings shed light on the diversity and complexity of the ubiquitination pathways.

Materials and methods

Recombinant protein expression and purification

Detailed creation of GST-Ubc13 and GST-Mms2 fusion constructs, their overexpression, protease cleavage, and purification have been described previously (McKenna et al., 2001). The GST-Uev1A and GST-Uev1B constructs were made by PCR amplification of *UEV1A* (obtained from Z.J. Chen, University of Texas Southwestern Medical Center, Dallas, TX) and *UEV1B* (*CROC1B*; obtained from S. Lin, Robert Wood Johnson Medical School, Piscataway, NJ) cDNA clones; the resulting fragments were cloned into pGEX6p (GE Healthcare). The GST-Ubc13K92R construct was created by site-directed mutagenesis and the GST-Uev1AΔ30 construct was made by PCR amplification that removes the NH_2-terminal 30-aa coding region from Uev1A. Each cloned insert was confirmed by DNA sequencing before further analysis. Fusion protein overexpression and purification were performed in a manner similar to that of GST-Ubc13 and GST-Mms2 (McKenna et al., 2001).

GST pull-down

GST pull-downs were performed using MicroSpin GST Purification Modules (GE Healthcare). 500 μl of bacterial crude cell extract containing GST-Mms2, GST-Uev1A, or GST-Uev1B was loaded and incubated in the purification module for 1 h at 4°C with gentle rocking. The module was then washed three times with 500 μl PBS (140 mM NaCl, 2.7 mM KCl, 10 mM Na_2HPO_4, and 1.8 mM KH_2PO_4, pH 7.3); 30 μg of purified Ubc13 in PBS was added and the incubation was continued for another hour at 4°C. The module was washed again three times with 500 μl PBS, and then 80 μl of reduced glutathione buffer (10 mM glutathione in 50 mM Tris-HCl, pH 8.0) was added to elute MicroSpin module-bound proteins. The elution samples were subjected to SDS-PAGE analysis.

Yeast two-hybrid analysis

The *hMMS2*, *UEV1A*, and *UEV1B* coding regions without stop codons were PCR amplified as BamHI–SalI fragments and cloned into pG4BD-1 (received from R.B. Brazas, University of California, San Francisco, San Francisco, CA) as COOH-terminal fusions to $Gal4_{BD}$. The *UBC13*-coding region was PCR amplified as an EcoRI–SalI fragment and cloned into pGAD424 (CLONTECH Laboratories, Inc.) as an NH_2-terminal fusion to $Gal4_{AD}$.

Yeast cells were grown in either rich YPD or synthetic SD minimal media at 30°C as described previously (Sherman et al., 1983) and were transformed with DNA by a LiAc protocol (Ito et al., 1983). Yeast strain PJ69-4A (*MAT**a** trp1-901 leu2-3,112 ura3-52 his3-200 gal4Δ gal80Δ LYS2::GAL1-HIS3 GAL2-ADE2 met::GAL7-lacZ*; received from P. James, University of Wisconsin, Madison, WI) was cotransformed with pG4BD-1– and pGAD424-based constructs, and the transformants were selected on SD-Trp-Leu plates. At least five independent transformants were picked from each plate and replicated onto SD-Trp-Leu-Ade to detect activation of the P_{GAL2}-ADE2 reporter gene or onto SD-Trp-Leu-His supplemented with various concentrations of 3-aminotriazole to measure activation of the P_{GAL1}-HIS3 reporter gene.

Functional analysis of human genes in yeast

A wild-type haploid *S. cerevisiae* strain, HK580-10D (*MATα ade-1 can1-100 his3 11,15 leu2-3, 112 trp1-1 ura3-1*), was received from H. Klein (New York University, New York, NY) and used as the recipient to delete the entire *MMS2* open reading frame by a one-step gene replacement method (Rothstein, 1983) using an *mms2Δ::HIS3* cassette generated through PCR amplification as previously described (Xiao et al., 1999). The resulting *mms2Δ* strain, WXY903, was transformed with two-hybrid plasmids carrying *hMMS2*, *UEV1A*, and *UEV1B* genes.

The gradient plate assay was performed as previously described (Xiao et al., 2000) to a semiquantitative measurement of relative MMS sensitivity.

mAb preparation

Recombinant human Ubc13 and Mms2 proteins were emulsified in Freund's incomplete adjuvant. Immediately before i.p. injection of BALB/c mice, the emulsion was dispersed with an equal volume of PBS containing 2% Tween 80 (injection volume per mouse of 0.8 ml). Repeat injections of antigen were given at minimum intervals of 3 wk over several months. Fusion cells were screened for secretion of a mAb with reactivity to either Ubc13 or Mms2 using standard enzyme immunoassay techniques in 96-well plates. Hybridomas 4E11 and 2H11 were isolated based on their ability to secrete mAbs recognizing Ubc13 and Mms2, respectively. Hybridoma cells ($\sim 10^6$) were injected into the peritoneal cavity of BALB/c mice that had received an i.p. injection of 0.3 ml of Freund's incomplete adjuvant 24 h before. Ascites fluid was collected as the mAb source.

Western blot analysis

Mouse NIH 3T3 cells were grown to log phase and lysed in Dulbecco's PBS (150 mM NaCl, 10 mM Na_2HPO_4, and 10 mM NaH_2PO_4, pH 7.4) with 1% SDS and the protease inhibitor cocktail for mammalian cells (Sigma-Aldrich). Total protein concentration was determined by the Bradford method using a commercial reagent from Bio-Rad Laboratories. Cell extracts or purified proteins were electrophoresed in 12% SDS-PAGE gels, transferred to PVDF membrane, incubated with mAb and a biotin-conjugated goat anti–mouse IgG secondary antibody (Sigma-Aldrich), followed by incubation with Streptavidin-HRP and DAB plus hydrogen peroxide for color development.

Constructs to express myc-tagged proteins

MMS2, *UEV1A*, and *UEV1AΔ30* open reading frames without stop codons were PCR-amplified as BamHI–XhoI fragments and then cloned into the BamHI–XhoI sites of pcDNA3.1/Myc-His(+)A (Invitrogen) so that the genes of interest are under the control of a CMV constitutive promoter and fused in frame with the myc-His_6 coding region at the COOH terminus.

RNAi and siRNA designs

RNAi constructs were created by cloning double-stranded oligonucleotides at XbaI and BbsI sites of the plasmid vector mU6pro (a gift from D. Turner, University of Michigan, Ann Arbor MI) as described previously (Yu et al., 2002). Double-stranded siRNAs were synthesized with 3′dTdT overhangs by Dharmacon. They were designed to recognize the target sequences as depicted in Fig. S3.

Cell culture, transfection, and treatments

Human and mouse cell lines were routinely grown in DME (Sigma-Aldrich) containing 4.5 g glucose and 10% horse serum (Invitrogen), with sodium bicarbonate reduced to 2.1 g/liter, in a humidified 5% CO_2 incubator. For transfection experiments, 50 μl of serum-free DME containing ~2 μg DNA and 1 μl Lipofectamine 2000 reagent (Invitrogen) was added to log-phase cells grown on 11 × 22-mm coverslips containing 100 μl of complete growth medium. After a 16-h incubation, the coverslips were returned to complete growth media and analyzed as specified. It was estimated that typical transfection efficiency was <10% using pcDNA3.1-derived constructs and >90% using RNAi constructs. For DNA damage treatment, log-phase cells were incubated continuously with CPT, followed by washing and immunocytochemistry (ICC). Microglia were isolated from newborn CD1 mice by aseptically pressing neopalia cleaned of meninges through 70-μm nitex mesh (BD Biosciences) and subsequently cultured in DME (high glucose) plus 10% horse serum as described previously (Hao et al., 1991). After 12-d culture, they were exposed to LPS and processed for ICC.

ICC methods

For routine ICC, cells were fixed in 4% formaldehyde in Dulbecco's PBS for 30 min, permeabilized by treating with 0.5% Triton X-100 for 5 min, and treated with a blocking solution containing 5% horse serum and 2% skim milk in PBS for 30 min. Primary antibodies used in this study include rabbit anti-Mre11 (1:200; Oncogene Research Products), rabbit anti-Rad51 (1:100; Santa Cruz Biotechnology, Inc.), mAb 2H11 (1:100), mAb 4E11 (1:100), mAb 9E10 (1:400; Sigma-Aldrich), Alexa546-conjugated mouse anti-BrdU (1:400; Molecular Probes), and rabbit anti-myc (1:400; Santa Cruz Biotechnology, Inc.). The green fluorescing Alexa488–conjugated anti–mouse (1:3,000; Molecular Probes) and the red fluorescing Alexa546-conjugated anti–rabbit (1:2,000; Molecular Probes) antibodies were used as secondary antibodies. The secondary antibody solution also contained 2 μg/ml DAPI to visualize the nucleus. Both primary and secondary antibodies were diluted in blocking solution and applied to cells for 30 min, each followed by three rinses with PBS over 30 min. The coverslips were then mounted in PBS and observed using an inverted fluorescence microscope (model IX70; Olympus) fitted with the appropriate filters. Digital images were taken using an RT Slider "Spot" camera and associated software (Diagnostic Instruments). Statistical data were compiled and analyzed using Microsoft Excel and GraphPad QuickCalcs Software (GraphPad Software, Inc.).

To visualize the incorporation of BrdU into DNA, cells were treated with 50 μg/ml DNase-free RNase A immediately after the permeabilization step, and the DNA was then denatured by treating cells with 2 N HCl for 15 min at 65°C before the blocking step. To differentiate the mouse mAbs 4E11 and 2H11 from mouse anti-BrdU, a modified procedure was developed. After the secondary Alexa488 anti–mouse antibody was applied to identify 4E11 and 2H11, coverslips were rinsed thoroughly (six changes of PBS over 1 h). The cells were again blocked by incubating with 2% normal mouse serum for 30 min to obstruct unoccupied anti–mouse Fab regions of bound Alexa488 anti–mouse antibody. Alexa546 anti-BrdU was then applied at a 1:400 dilution for 15 min. To visualize damage-induced nuclear foci (Tomilin et al., 2001), in situ cell fractionation was performed before fixation by treating cells with 0.4% NP-40 in PBS for 3.5 min with gentle agitation.

NF-κB luciferase reporter and NEMO ubiquitination assays

HEK 293T cells were plated in 6-well plates 18 h before transfection. For siRNA delivery, cells were transfected with 25 nmol of the indicated siRNA, using Lipofectamine 2000 (Invitrogen). 24 h after the first transfection, the cells were transfected again with the same amount of siRNA together with the indicated expression plasmids. Approximately 36 h after the second transfection, the cells were collected and used for different experiments. NF-κB reporter activity was measured using a Dual-Luciferase Reporter Assay System (Promega) according to the manufacturer's protocol. Immunoblot analysis of NEMO ubiquitination was performed as described previously (Zhou et al., 2004).

In vitro ubiquitination assay

A 0.5-ml conjugation reaction containing 20 nM Uba1, 2.5 μM ^{35}S-labeled Ub, and 250 nM Ubc13 in an ATP cocktail (10 mM Hepes, pH 7.5, 5 mM $MgCl_2$, 5 mM ATP, and 0.6 U/ml inorganic phosphatase) were incubated at 30°C for 90 min. The concentration of each component is noted in the figure legends. Reactions were terminated by the addition of TCA to a final concentration of 10% and processed for a 12% SDS-PAGE analysis by autoradiography.

Image acquisition and processing

All photographic images were taken through a microscope (model IX70; Olympus) with a camera (SPOT RT Slider; Diagnostic Instruments) at RT. Fluorochromes used include Alexa488 (green; Molecular Probes), Alexa-546 (red; Molecular Probes), and DAPI (blue; Sigma-Aldrich). For Figs. 5 and 7, an LC PlanFL 40×/0.60 (air) objective (Olympus) was used. For Fig. 4 and Fig. S2, an UPlanFLN 60×/1.25 oil immersion objective (Olympus) was used. Images were acquired using Image-Pro Plus version 4.1 software and compiled using Adobe Photoshop version 6. In each plate, photographs were cropped and each Fluorochrome adjusted identically for brightness and contrast to represent the observed images. In Fig. 7, the cyan channel was adjusted identically in all panels to accentuate the merged layer.

Online supplemental material

Fig. S1 shows quantitative analysis of nuclear foci–containing cells after CPT treatment. Fig. S2 shows cellular localization of Mms2-myc and Uev1-myc proteins. Fig. S3 shows RNAi and siRNA sequences. Online supplemental material is available at http://www.jcb.org/cgi/content/full/jcb.200502113/DC1.

We thank Drs. R.B. Brazas, Z.J. Chen, P. James, H. Klein, S. Lin, and D. Turner for reagents and Michelle Hanna for proofreading the manuscript.

This work was supported by the Canadian Institutes of Health Research (operating grant MOP-53240) and the Cancer Research Society Inc. (grant to W. Xiao). P.L. Andersen is supported by a University of Saskatchewan College of Medicine Graduate Scholarship and L. Pastushok is a Natural Sciences and Engineering Research Council of Canada scholar.

Submitted: 18 February 2005
Accepted: 20 July 2005

References

Andegeko, Y., L. Moyal, L. Mittelman, I. Tsarfaty, Y. Shiloh, and G. Rotman. 2001. Nuclear retention of ATM at sites of DNA double strand breaks. *J. Biol. Chem.* 276:38224–38230.

Bonaiuto, C., P.P. McDonald, F. Rossi, and M.A. Cassatella. 1997. Activation of nuclear factor-κB by β-amyloid peptides and interferon-γ in murine microglia. *J. Neuroimmunol.* 77:51–56.

Bothos, J., M.K. Summers, M. Venere, D.M. Scolnick, and T.D. Halazonetis. 2003. The Chfr mitotic checkpoint protein functions with Ubc13-Mms2 to form Lys63-linked polyubiquitin chains. *Oncogene.* 22:7101–7107.

Brinkmann, U., M. Gallo, M.H. Polymeropoulos, and I. Pastan. 1996. The human CAS (cellular apoptosis susceptibility) gene mapping on chromosome 20q13 is amplified in BT474 breast cancer cells and part of aberrant chromosomes in breast and colon cancer cell lines. *Genome Res.* 6:187–194.

Broomfield, S., B.L. Chow, and W. Xiao. 1998. *MMS2*, encoding a ubiquitin-conjugating-enzyme-like protein, is a member of the yeast error-free postreplication repair pathway. *Proc. Natl. Acad. Sci. USA.* 95:5678–5683.

Brown, M., Y. Zhu, S.M. Hemmingsen, and W. Xiao. 2002. Structural and functional conservation of error-free DNA postreplication repair in *Schizosaccharomyces pombe*. *DNA Repair (Amst.).* 1:869–880.

Brummelkamp, T.R., S.M. Nijman, A.M. Dirac, and R. Bernards. 2003. Loss of the cylindromatosis tumour suppressor inhibits apoptosis by activating NF-κB. *Nature.* 424:797–801.

Brusky, J., Y. Zhu, and W. Xiao. 2000. *UBC13*, a DNA-damage-inducible gene, is a member of the error-free postreplication repair pathway in *Saccharomyces cerevisiae*. *Curr. Genet.* 37:168–174.

Chau, V., J.W. Tobias, A. Bachmair, D. Marriott, D.J. Ecker, D.K. Gonda, and A. Varshavsky. 1989. A multiubiquitin chain is confined to specific lysine in a targeted short-lived protein. *Science.* 243:1576–1583.

Deng, L., C. Wang, E. Spencer, L. Yang, A. Braun, J. You, C. Slaughter, C. Pickart, and Z.J. Chen. 2000. Activation of the IκB kinase complex by TRAF6 requires a dimeric ubiquitin-conjugating enzyme complex and a unique polyubiquitin chain. *Cell.* 103:351–361.

Dixit, V., and T.W. Mak. 2002. NF-κB signaling. Many roads lead to Madrid. *Cell.* 111:615–619.

Doss-Pepe, E.W., L. Chen, and K. Madura. 2005. α-Synuclein and Parkin contribute to the assembly of ubiquitin lysine 63-linked multiubiquitin chains. *J. Biol. Chem.* 280:16619–16624.

El-Rifai, W., J.C. Harper, O.W. Cummings, E.R. Hyytinen, H.F. Frierson Jr., S. Knuutila, and S.M. Powell. 1998. Consistent genetic alterations in xenografts of proximal stomach and gastro-esophageal junction adenocarcinomas. *Cancer Res.* 58:34–37.

Franko, J., C. Ashley, and W. Xiao. 2001. Molecular cloning and functional char-

acterization of two murine cDNAs which encode Ubc variants involved in DNA repair and mutagenesis. *Biochim. Biophys. Acta.* 1519:70–77.

Galan, J.M., and R. Haguenauer-Tsapis. 1997. Ubiquitin lys63 is involved in ubiquitination of a yeast plasma membrane protein. *EMBO J.* 16:5847–5854.

Hao, C., A. Richardson, and S. Fedoroff. 1991. Macrophage-like cells originate from neuroepithelium in culture: characterization and properties of the macrophage-like cells. *Int. J. Dev. Neurosci.* 9:1–14.

Haracska, L., C.A. Torres-Ramos, R.E. Johnson, S. Prakash, and L. Prakash. 2004. Opposing effects of ubiquitin conjugation and SUMO modification of PCNA on replicational bypass of DNA lesions in *Saccharomyces cerevisiae*. *Mol. Cell. Biol.* 24:4267–4274.

Hatakeyama, S., and K.I. Nakayama. 2003. U-box proteins as a new family of ubiquitin ligases. *Biochem. Biophys. Res. Commun.* 302:635–645.

Hoege, C., B. Pfander, G.L. Moldovan, G. Pyrowolakis, and S. Jentsch. 2002. *RAD6*-dependent DNA repair is linked to modification of PCNA by ubiquitin and SUMO. *Nature.* 419:135–141.

Hofmann, R.M., and C.M. Pickart. 1999. Noncanonical *MMS2*-encoded ubiquitin-conjugating enzyme functions in assembly of novel polyubiquitin chains for DNA repair. *Cell.* 96:645–653.

Ito, H., Y. Fukuda, K. Murata, and A. Kimura. 1983. Transformation of intact yeast cells treated with alkali cations. *J. Bacteriol.* 153:163–168.

Kallioniemi, A., O.P. Kallioniemi, J. Piper, M. Tanner, T. Stokke, L. Chen, H.S. Smith, D. Pinkel, J.W. Gray, and F.M. Waldman. 1994. Detection and mapping of amplified DNA sequences in breast cancer by comparative genomic hybridization. *Proc. Natl. Acad. Sci. USA.* 91:2156–2160.

Kannouche, P.L., J. Wing, and A.R. Lehmann. 2004. Interaction of human DNA polymerase η with monoubiquitinated PCNA: a possible mechanism for the polymerase switch in response to DNA damage. *Mol. Cell.* 14:491–500.

Koegl, M., T. Hoppe, S. Schlenker, H.D. Ulrich, T.U. Mayer, and S. Jentsch. 1999. A novel ubiquitination factor, E4, is involved in multiubiquitin chain assembly. *Cell.* 96:635–644.

Kovalenko, A., C. Chable-Bessia, G. Cantarella, A. Israel, D. Wallach, and G. Courtois. 2003. The tumour suppressor CYLD negatively regulates NF-κB signalling by deubiquitination. *Nature.* 424:801–805.

Li, Z., W. Xiao, J.J. McCormick, and V.M. Maher. 2002. Identification of a protein essential for a major pathway used by human cells to avoid UV-induced DNA damage. *Proc. Natl. Acad. Sci. USA.* 99:4459–4464.

Lim, K.L., K.C. Chew, J.M. Tan, C. Wang, K.K. Chung, Y. Zhang, Y. Tanaka, W. Smith, S. Engelender, C.A. Ross, et al. 2005. Parkin mediates nonclassical, proteasomal-independent ubiquitination of synphilin-1: implications for Lewy body formation. *J. Neurosci.* 25:2002–2009.

Ma, L., S. Broomfield, C. Lavery, S.L. Lin, W. Xiao, and S. Bacchetti. 1998. Up-regulation of *CIR1/CROC1* expression upon cell immortalization and in tumor-derived human cell lines. *Oncogene.* 17:1321–1326.

Maser, R.S., O.K. Mirzoeva, J. Wells, H. Olivares, B.R. Williams, R.A. Zinkel, P.J. Farnham, and J.H. Petrini. 2001. Mre11 complex and DNA replication: linkage to E2F and sites of DNA synthesis. *Mol. Cell. Biol.* 21:6006–6016.

McKenna, S., L. Spyracopoulos, T. Moraes, L. Pastushok, C. Ptak, W. Xiao, and M.J. Ellison. 2001. Noncovalent interaction between ubiquitin and the human DNA repair protein Mms2 is required for Ubc13-mediated polyubiquitination. *J. Biol. Chem.* 276:40120–40126.

McKenna, S., T. Moraes, L. Pastushok, C. Ptak, W. Xiao, L. Spyracopoulos, and M.J. Ellison. 2003. An NMR-based model of the ubiquitin-bound human ubiquitin conjugation complex Mms2-Ubc13. The structural basis for lysine 63 chain catalysis. *J. Biol. Chem.* 278:13151–13158.

Moraes, T.F., R.A. Edwards, S. McKenna, L. Pastushok, W. Xiao, J.N. Glover, and M.J. Ellison. 2001. Crystal structure of the human ubiquitin conjugating enzyme complex, hMms2-hUbc13. *Nat. Struct. Biol.* 8:669–673.

Pastushok, L., and W. Xiao. 2004. DNA postreplication repair modulated by ubiquitination and sumoylation. *Adv. Protein Chem.* 69:279–306.

Pickart, C.M. 2001a. Mechanisms underlying ubiquitination. *Annu. Rev. Biochem.* 70:503–533.

Pickart, C.M. 2001b. Ubiquitin enters the new millennium. *Mol. Cell.* 8:499–504.

Rothofsky, M.L., and S.L. Lin. 1997. CROC-1 encodes a protein which mediates transcriptional activation of the human FOS promoter. *Gene.* 195:141–149.

Rothstein, R.J. 1983. One-step gene disruption in yeast. *Methods Enzymol.* 101:202–211.

Ryan, A.J., S. Squires, H.L. Strutt, and R.T. Johnson. 1991. Camptothecin cytotoxicity in mammalian cells is associated with the induction of persistent double strand breaks in replicating DNA. *Nucleic Acids Res.* 19:3295–3300.

Sakamoto, S., K. Nishikawa, S.J. Heo, M. Goto, Y. Furuichi, and A. Shimamoto. 2001. Werner helicase relocates into nuclear foci in response to DNA damaging agents and co-localizes with RPA and Rad51. *Genes Cells.* 6:421–430.

Sancho, E., M.R. Vila, L. Sanchez-Pulido, J.J. Lozano, R. Paciucci, M. Nadal, M. Fox, C. Harvey, B. Bercovich, N. Loukili, et al. 1998. Role of UEV-1, an inactive variant of the E2 ubiquitin-conjugating enzymes, in in vitro differentiation and cell cycle behavior of HT-29-M6 intestinal mucosecretory cells. *Mol. Cell. Biol.* 18:576–589.

Savelieva, E., C.D. Belair, M.A. Newton, S. DeVries, J.W. Gray, F. Waldman, and C.A. Reznikoff. 1997. 20q gain associates with immortalization: 20q13.2 amplification correlates with genome instability in human papillomavirus 16 E7 transformed human uroepithelial cells. *Oncogene.* 14:551–560.

Sherman, F., G.R. Fink, and J. Hicks. 1983. Methods in Yeast Genetics. Cold Spring Harbor Laboratory Press, Cold Spring Harbor, NY. 186 pp.

Shi, C.S., and J.H. Kehrl. 2003. Tumor necrosis factor (TNF)-induced germinal center kinase-related (GCKR) and stress-activated protein kinase (SAPK) activation depends upon the E2/E3 complex Ubc13-Uev1A/TNF receptor-associated factor 2 (TRAF2). *J. Biol. Chem.* 278:15429–15434.

Spence, J., R.R. Gali, G. Dittmar, F. Sherman, M. Karin, and D. Finley. 2000. Cell cycle-regulated modification of the ribosome by a variant multiubiquitin chain. *Cell.* 102:67–76.

Stelter, P., and H.D. Ulrich. 2003. Control of spontaneous and damage-induced mutagenesis by SUMO and ubiquitin conjugation. *Nature.* 425:188–191.

Sun, L., and Z.J. Chen. 2004. The novel functions of ubiquitination in signaling. *Curr. Opin. Cell Biol.* 16:119–126.

Sun, L., L. Deng, C.K. Ea, Z.P. Xia, and Z.J. Chen. 2004. The TRAF6 ubiquitin ligase and TAK1 kinase mediate IKK activation by BCL10 and MALT1 in T lymphocytes. *Mol. Cell.* 14:289–301.

Tanner, M.M., M. Tirkkonen, A. Kallioniemi, C. Collins, T. Stokke, R. Karhu, D. Kowbel, F. Shadravan, M. Hintz, W.L. Kuo, et al. 1994. Increased copy number at 20q13 in breast cancer: defining the critical region and exclusion of candidate genes. *Cancer Res.* 54:4257–4260.

Tomilin, N.V., L.V. Solovjeva, M.P. Svetlova, N.M. Pleskach, I.A. Zalenskaya, P.M. Yau, and E.M. Bradbury. 2001. Visualization of focal nuclear sites of DNA repair synthesis induced by bleomycin in human cells. *Radiat. Res.* 156:347–354.

Tsao, Y.P., A. Russo, G. Nyamuswa, R. Silber, and L.F. Liu. 1993. Interaction between replication forks and topoisomerase I-DNA cleavable complexes: studies in a cell-free SV40 DNA replication system. *Cancer Res.* 53:5908–5914.

VanDemark, A.P., R.M. Hofmann, C. Tsui, C.M. Pickart, and C. Wolberger. 2001. Molecular insights into polyubiquitin chain assembly: crystal structure of the Mms2/Ubc13 heterodimer. *Cell.* 105:711–720.

Villalobo, E., L. Morin, C. Moch, R. Lescasse, M. Hanna, W. Xiao, and A. Baroin-Tourancheau. 2002. A homologue of CROC-1 in a ciliated protist (*Sterkiella histriomuscorum*) testifies to the ancient origin of the ubiquitin-conjugating enzyme variant family. *Mol. Biol. Evol.* 19:39–48.

Wang, C., L. Deng, M. Hong, G.R. Akkaraju, J. Inoue, and Z.J. Chen. 2001. TAK1 is a ubiquitin-dependent kinase of MKK and IKK. *Nature.* 412:346–351.

Watanabe, K., S. Tateishi, M. Kawasuji, T. Tsurimoto, H. Inoue, and M. Yamaizumi. 2004. Rad18 guides poleta to replication stalling sites through physical interaction and PCNA monoubiquitination. *EMBO J.* 23:3886–3896.

Wong, B.R., F. Parlati, K. Qu, S. Demo, T. Pray, J. Huang, D.G. Payan, and M.K. Bennett. 2003. Drug discovery in the ubiquitin regulatory pathway. *Drug Discov. Today.* 8:746–754.

Xiao, W., S.L. Lin, S. Broomfield, B.L. Chow, and Y.F. Wei. 1998. The products of the yeast *MMS2* and two human homologs (*hMMS2* and *CROC-1*) define a structurally and functionally conserved Ubc-like protein family. *Nucleic Acids Res.* 26:3908–3914.

Xiao, W., B.L. Chow, T. Fontanie, L. Ma, S. Bacchetti, T. Hryciw, and S. Broomfield. 1999. Genetic interactions between error-prone and error-free postreplication repair pathways in *Saccharomyces cerevisiae*. *Mutat. Res.* 435:1–11.

Xiao, W., B.L. Chow, S. Broomfield, and M. Hanna. 2000. The *Saccharomyces cerevisiae RAD6* group is composed of an error-prone and two error-free postreplication repair pathways. *Genetics.* 155:1633–1641.

Yu, J.Y., S.L. DeRuiter, and D.L. Turner. 2002. RNA interference by expression of short-interfering RNAs and hairpin RNAs in mammalian cells. *Proc. Natl. Acad. Sci. USA.* 99:6047–6052.

Zhou, H., I. Wertz, K. O'Rourke, M. Ultsch, S. Seshagiri, M. Eby, W. Xiao, and V.M. Dixit. 2004. Bcl10 activates the NF-κB pathway through ubiquitination of NEMO. *Nature.* 427:167–171.